International Digital Organization for Scientific Research ISSN: 2579-079X
IDOSR JOURNAL OF SCIENCE AND TECHNOLOGY 6(1):85-94, 2021.

Characterizing the Physical Properties of A 6.7 Ghz Methanol Maser Star Forming Region G338.93-0.06

Okongwu, O[1]., Mba, C .E[2]., Muallim, Y[1,]. and Chima, A.I[1]
[1]Department of Industrial Physics, Enugu State University of Science and Technology,
[2]NASRDA-Center for Basic Space Science, Ebirimmiri Agu Umuakashi Nsukka
Corresponding email address: Abraham.chima@esut.edu.ng.08066922634

ABSTRACT

This work studied the spectral energy distribution (SED) of G338.93.0.06 and uses the model to estimate the physical properties of the source such as the stellar parameters (Stellar mass, temperature, age, radius, luminosity) the envelope parameters (mass, envelope radius, accretion rate, circumstellar extinction, cavity angle) and the disk parameters (mass,size,scale height, inner/outer radius) A combined infrared data from GLIMPSE, MIPSGAL, Hi-GAL and ATLASGAL surveys were used to perform the SED with a correlation coefficient of 0.6489. The spectral index obtained from the power law (α~ 1.7964 > 1) signifies that G338.93-0.06 is a Class I young stellar object that is deeply embedded in the molecular cloud. The physical properties of G338.93-0.06 revealed a class-I YSO with a relatively young core and an intermediate mass of 3.95 $M_{\odot}$, the star is at its young age of 2.426×10^{4} yrwith an effective temperature of 4.38×10^{3} K. A broader SED of the source shows mid-infrared and near-infrared excess emanating from large amounts of circum-protostellar dust. With an envelope radius of 1.058×10^{4} AU, surrounding the protostar, isothermal free-fall accretion is expected to continue above the adiabatic protostar core and the density and temperature will continue to increase.
Keywords: Spectral index, circum-protostellar dust and adiabatic protostar core

INTRODUCTION

Stars are bright, round objects that are mostly made up of gases that are held together by gravity [1]. Nuclear fusion - a reaction in which hydrogen is fusioned into helium at the core of a star and energy is released that travels through the star's interior and eventually radiates into space – produces these gases, which are mostly hydrogen and helium [2]; [3]. They are major components of the astronomical world due to their unique nature. Star clusters, globular clusters, and galaxies are made up of them. Galaxies, such as the Milky Way and Andromeda, are formed by billions of them.Stars emerge in the sky as single points of light. They exhibit some colorfulbehavior and traits when observed via telescopes. Some are single point sources, while others are extended pairs of binary or multiple stars revolving around a common barycenter [4].

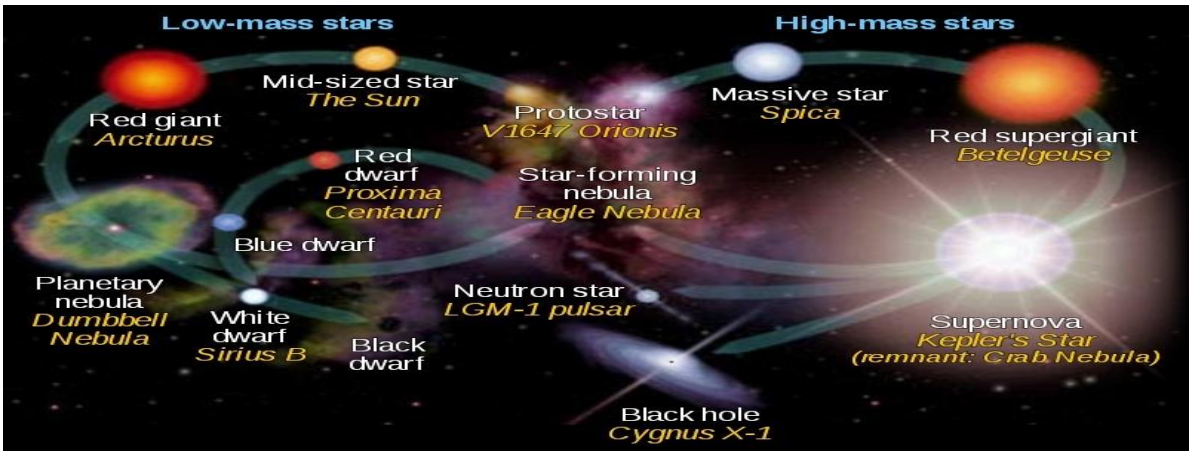

Figure 1: Stellar evolution of low-mass (left cycle) and high-mass (right cycle). Source: Wikipedia

Stars are produced from interstellar dust and gas that is gravitationally bonded in such a way that the internal pressure compresses the core, according to stellar evolution research [5]. The MilkyWay and other galaxies rely heavily on interstellar gas and dust [6]. Star creation propagates via the action of shock waves created by stellar winds and supernovae traversing the gas that makes up the interstellar medium, according to the stochastic self-propagating star formation model [7].

Star formation can produce stars of various sizes, ranging from low mass to high mass, depending on the starting mass function. Figure 1.1 depicts the evolution of stars as they grow in size. Our Sun is a star with a low mass. Over the last century, the study of stars (stellar objects) has raised new questions about the mechanisms that contribute to their birth [8].

If a star's mass is at least eight times that of the Sun, it is called massive. The mass of the Sun is 6.4 1024 kg. Massive stars, according to [9], are characterized by heavy elements and UV radiation. They are a key source of mixing and turbulence in galaxies' interstellar medium (ISM) through a mixture of winds, large outflows, expanding HII regions, and supernova explosions. Galactic dynamos are propelled by their turbulence, which is combined with differential rotation. Galactic magnetic fields are created in the Milky Way, which interact with supernova shock fronts to accelerate high-energy cosmic rays.

Massive stars have a significant impact on the development of stars and planets, as well as the physical, chemical, and morphological structure of galaxies.

Despite the fact that big stars play a prominent role in determining galaxy structure and evolution, our knowledge of their genesis and early history is limited. This is due to a variety of factors. Observing high-mass stars during critical early creation phases is difficult due to substantial dust extinction. They are extremely rare. They evolve swiftly, with crucial evolutionary phases lasting only a few years. The theoretical issue is incredibly difficult to solve.Finally, huge stars are rarely (if ever) born in isolation; gravitational interactions, tremendous outflows and winds, ionizing radiation, and supernovae all compound the complicated influence of the forming star on its local environment [10].

Massive stars (those with a mass greater than eight times that of the Sun) are the most powerful actors in the Galaxy. Despite their limited number, they are responsible for the vast majority of visible light in the Galaxy.They have a significant impact on the galactic environment by ionizing the interstellar medium with powerful ultraviolet radiation and altering the makeup of the interstellar medium by producing heavy elements via supernovae explosions in their very brief lifespan.

Low-mass stars outnumber big stars in the stellar population of galaxies.

High mass stars, on the other hand, have a significantly greater impact on the galaxy's environment than their low mass counterparts. High-mass stars produce powerful stellar winds, emit intense ultraviolet radiation that causes HII areas, and die in enormous supernova explosions that can outshine the host galaxy. Despite the importance of massive stars, our knowledge of their creation process is currently restricted when compared to that of low mass stars. Several causes contribute to this: huge stars remain deeply immersed in the parent molecular cloud for a long time after they reach the zero age main sequence, which is due in part to the short timescales required in massive star creation and evolution. Massive star formation regions are more distant and severely veiled (occasionally even in mid infrared wavelengths).Furthermore, because big stars tend to originate in clusters and have a strong interaction with their surroundings, interpreting observational data is difficult [11]. Molecules like hydroxyl-OH, water-H_2O, and methanol-CH_3OH, which are commonly discovered as masers in interstellar space, are known to be associated with high-mass star-forming regions. In contrast to their OH and water counterparts, which are also observed toward other astronomical objects such as late-type stars, Class II methanol masers are unique among these in that they are only observed

toward high-mass star formation areas [12].

When these masers are identified, they generally have several emission lines that are projected against ultra-compact HII areas [13]. The bulks of methanol masers, on the other hand, emit only in the 6.7GHz transition and have no observable HII areas. Recent observations have revealed that sources that do not emit centimetre radio continuum emission are associated with millimetre [14] and sub-millimetre [15] sources, have a spectral energy distribution consistent with them being deeply embedded [16], and are associated with a very early stage of the star formation process.

Masers have the potential to be powerful probes of the high-mass star formation process, but they must first be understood in the context in which they form. To explain the high brightness temperatures observed, theoretical models of Class II methanol masers evoke stimulation to the second torsional state from the radiative field of heated dust at sub-millimetre and far-infrared (FIR) wavelengths. In searches for Infrared Astronomical Satellite (IRAS) sources that match the [17] criteria for having ultra-compact HII regions, many methanol masers have been discovered.

However, in many cases, the masers are not directly associated with the IRAS sources, but rather with the larger star formation region.

In this study we are going to construct spectral energy distribution (SED) model for G338.93-0.06 and use the model to estimate its physical properties such as its:stellar mass, temperature, age, radius, luminosity,Accretion rate, circumstellar extinction, cavity angle, and scale height.

The goal of this research is to learn more about the evolutionary stage and physical features of the star-forming area G338.93-0.06 by using multiwavelength data. The science of employing or combining two or more wavebands of the electromagnetic spectrum to analyze an astronomical object is known as multiwavelength studies. Some objects emit light in a variety of wavelengths, each of which reveals a particular aspect of their makeup and behavior. Objects that are absolutely invisible at one wavelength can be seen at a different wavelength, giving astronomers a deeper understanding of the Universe. Depending on the temperature of the object, some astronomical objects emit predominantly infrared, visible light, and radio. However, molecular clouds are more visible in the radio, microwave, and infrared frequencies due to their composition, which is usually characterized by a high dust density that shields most of the radiation.

Source of Data

For the study of the physical properties of G338.93-0.06, data was collected from multiple surveys such as GLIMPSE, MIPSGAL and Hi-GAL.

METHODS

The python programming language was used for all of the analysis in this project. Python is a multifunctional and user-friendly programming language popular among scientists. To execute the analysis, fit the SED, and create the plot images, a number of python tools were utilized, including numpy, pandas, matplotlib, scipy, astropy, and sedfitter.

RESULTS

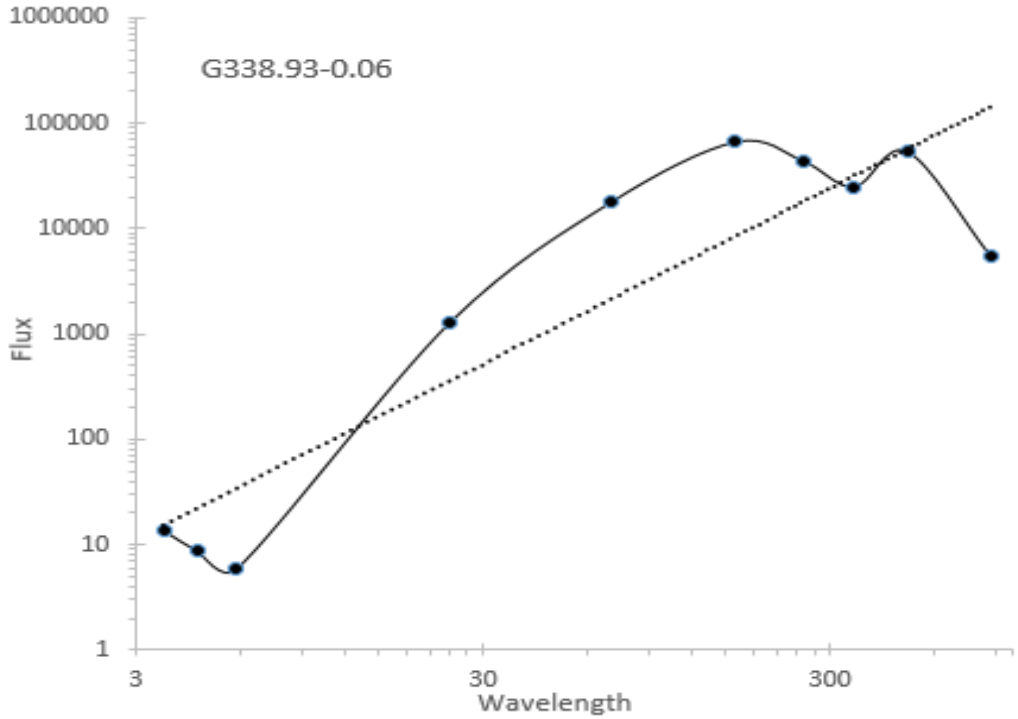

Figure 2: Spectral Energy distribution of G338.93-0.06

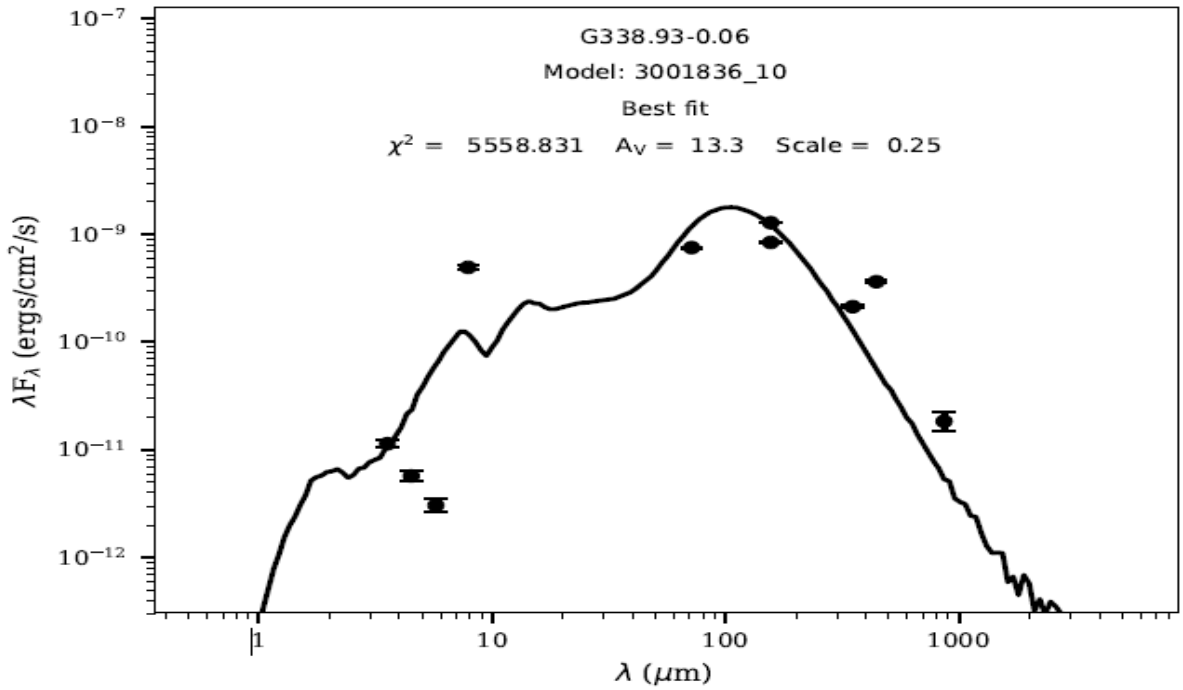

Figure 3: The spectral energy distribution fitting of G338.93-0.06

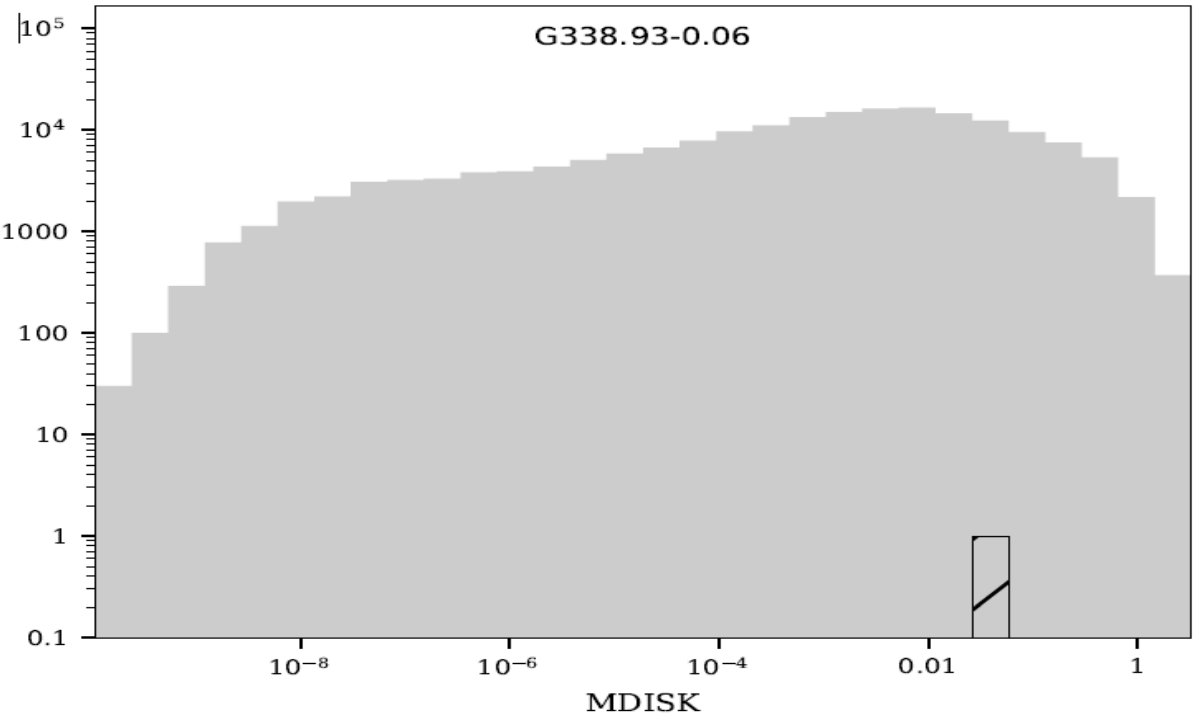

Figure 4: Modelled disk mass of G338.93-0.06

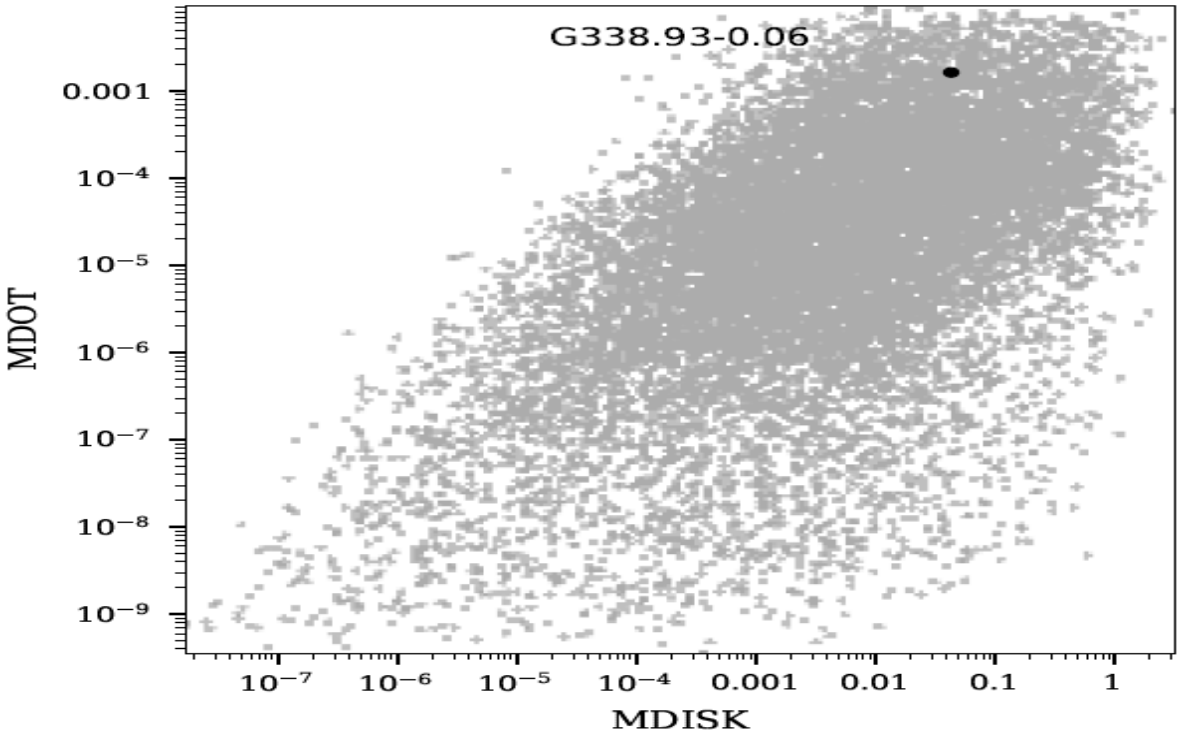

Figure 5: Disk mass density distribution of G338.93-0.06

DISCUSSION

Spectral Energy Distribution

To obtain a spectral energy distribution for G338.9-0.06, fluxes were obtained at IRAC, MIPSGAL, Hi-GAL and SCUBA wavebands from Vizier at not more than a radius of 1 arcminute. These fluxes are presented in Table 1 with their uncertainties. Both the fluxes and its uncertainties are in milli-Jansky (mJy) whereas wavelengths are in (microns, μm). There was no flux data for IRAC 8.0 μm waveband.

Table 1: Fluxes obtained at different wavelengths

Wavelength, λ (μm)	Flux (mJy)	Uncertainty (mJy)	Filters
3.60	13.490	0.9071	I1
4.50	8.630	1.040	I2
5.80	5.880	0.7830	I3
8.00	0.000	0.000	I4
24.00	1297.255	71.037	M1
70.00	17923.700	267.000	M2
160.00	66651.700	714.000	M3
250.00	43719.000	641.000	N1
350.00	24875.000	684.000	N1
500.00	53625.000	1940.000	N2
870.00	5390.000	1060.000	N4

As the wavelength increases, the flux increases and peaks at 160 μm where the source records a flux of records a 66651.700 mJy and drops significantly afterwards. The data in Table 1 is used in combination with the respective filters. Wavelengths 250.0 and 350.0μm both share the same filters owing to the fact that N1 filters covers both wavelength ranges. These data are used in producing a piece-wise spectral energy distribution (SED) to show a somewhat blackbody curves which indicates the amount of energy emitted by the source as the wavelengths varies with the temperature of the source. The emission from this source is similar to a blackbody. Figure 2 shows the spectral energy distribution of G338.93-0.06 in logarithmic scale with a power law fitting showing it is positively correlated with a correlation coefficient of 0.6489. From the SED, the source double peaked at 160.0 and 500.0 μm indicating it is still evolving and in a very young stage. The spectral index obtained from the power law is: $F_\lambda = 1.7964\lambda^{1.6671}$ with a spectral index (slope) of 1.7964. The spectral index usually defined as:

$$\alpha = \frac{\partial \log(F_\lambda)}{\partial \log \lambda} \qquad 1.1$$

Where F_λ is the flux of the young stellar object and λ is the wavelength of the YSO. Spectral index is commonly used in describing the evolutionary stage of young stellar objects. According to [18], young stellar objects with spectral index greater than 0 ($\alpha > 0$) are Class I YSOs. Class I YSOs are deeply embedded sources, with positive-IR spectral index, emitting in the mm and submm wavelengths.

SED FITTING

A full-fledged spectral energy distribution of G338.93-0.06 is shown in Figure 2. This was achieved using the sed-fitter module in python. Using data from Table 1 and their corresponding filters, the SED fitting was performed with a grid of 200,000 YSO pre-computed SEDs [19]. The models consist of pre-main-sequence stars with different combinations of axisymmetric circumstellar disks covering a wide

range of stellar masses (from 0.1 to 50 $M_{\odot}$) and evolutionary stages from the early envelope in-fall stage to the late disk-only stage. The grid consists of 20,000 YSO models, with spectral energy distributions (SEDs) and polarization spectra computed at 10 viewing angles for each model, resulting in a total of 200,000 SEDs [20].

The SED fitting for G338.93-0.06 (Figure 2) is characterized as a class-I young stellar object based on its spectral index. The physical properties of the source estimated from the fitting is listed in Table. 2.

Table 2: Physical properties of G338.93-0.06

S/N	Parameters	Value
	Central source(stellar) properties	
1	Stellar mass	3.95 $M_{\odot}$
2	Age of Star	2.426×10^{4} yr
3	Radius	20.03 $R_{\odot}$
4	Temperature	4.38×10^{3} K
5	Luminosity	1.925×10^{2} $L_{\odot}$
6	Core size	14.71 pc
	Envelope properties	
7	Mass loss (accretion) rate	1.632×10^{-3} yr^{-1}
8	Envelope radius	1.058×10^{4} AU
9	Envelope Cavity angle	6.132°
10	Cavity density	2.069×10^{-20} gcm^{-3}
11	Inclination	18.19°
12	Ambient density	2.498×10^{-21} gcm^{-3}
13	Opacity	1.257×10^{3}
	Disk properties	
14	Disk mass (gas + dust)	4.334×10^{-2} $M_{\odot}$
15	Disk outer radius	14.71 AU
16	Disk inner radius	14.58 AU
17	Disk minimum size	13.64 AU
18	Disk scale height factor	0.8598
19	Disk (disk mass accretion rate for outer radius	1.209×10^{-5} $M_{\odot}yr^{-1}$

To describe the evolutionary stages of YSOs using sedfitter, [21] adopted a Stage classification analogous to the Class scheme, but referring to the actual evolutionary stage of the object, based on its physical properties rather than properties of its SED. With an envelope mass accretion rate of $1.632\times10^{-3}yr^{-1}$ (> 10^{-6} yr^{-1}), G338.93-0.06 is a Stage I YSO.

The left skewed unimodal distribution of disk mass is shown in Figure 3. The gas disk (with a mass of 4.334×10^{-2} $M_{\odot}$) is spread around the core with no significant holes present between the inner and the outer disk. On the other hand, the inclination is without a large steep while Figure 4 reveals dust opacity that show a little dispersed disk mass.

Summary

Stars normally form in an evolutionary order, and YSOs' physical and structural features evolve as well. The physical and structural evolution of pre-main sequence stars, as well as the evolution of star clusters, can be described using analytical methods such as fitting SEDs on a star formation region. Because dust in disks and envelopes is heated by irradiation from the star and accretion shocks at the stellar surface, effective temperature and luminosity are the most important parameters in understanding the evolutionary status of the central source. They also play a key role in the physical properties of disks and envelopes.With a central core mass of 3.95 $M_{\odot}$, G338.93-0.06 is an intermediate mass YSO with a radius of 20.03 R⊙. The stellar temperature of the source is 4.38×10^{3} K with a luminosity of 1.925×10^{2}L⊙. Similarly, the envelope surrounding the central YSO source is

large with a radius of 1.058×10^{4} AU with an estimated accretion rate of 1.632×10^{-3} $M_{\odot}yr^{-1}$. The large envelope size signifies that G338.93-0.06 accretion is spherical on the size-scales of dense core [22]. The disk properties such as disk mass, inner radius and outer radius and accretion rate were estimated as 4.334×10^{-2} $M_{\odot}$, 14.58 AU, 14.71 AU and 1.209×10^{-5} $M_{\odot}yr^{-1}$ respectively.

Spectral index is a key parameter estimated from the spectral energy distribution and used in classifying the class of a young stellar object. Giving the spectral index value of 1.7964 (>1), it is clear from [23] that G338.93-0.06 is a class-I YSO. This type of YSOs is characterized with infalling envelope (~10^{4} AU) and optically thick disk (around 100 AU), luminosity from disk accretion shock, bipolar-out-flows, infrared emission. With an envelope radius of 1.058×10^{4} AU, it is clear that a protostar has formed within the core.

Isothermal free-fall accretion, on the other hand, is projected to proceed above the adiabatic protostar core, increasing density and temperature. The stellar wind is rising and the bi-polar jet mass is extending at this stage of the source. Figure 3 displays a broader SED with excess in the mid-infrared and near-infrared. Large volumes of circum-protostellar dust are responsible for the excess infrared.

The spectral index obtained from the power law (α~ 1.7964 > 1) signifies that G338.93-0.06 is a Class I young stellar object that is deeply embedded in the molecular cloud. The physical properties of G338.93-0.06 revealed a class-I YSO with a relatively young core and an intermediate mass of 3.95 $M_{\odot}$, the star is at its young age of 2.426×10^{4} yrwith an effective temperature of 4.38×10^{3} K. A broader SED of the source shows mid-infrared and near-infrared excess emanating from large amounts of circum-protostellar dust. With an envelope radius of 1.058×10^{4} AU, surrounding the protostar, isothermal free-fall accretion is expected to continue above the adiabatic protostar core and the density and temperature will continue to increase.

CONCLUSION

The multiwavelength approach has become one of the useful methods of studying astronomical sources. Using the mid and near infrared surveys data from GLIMPSE, MIPSGAL, Hi-GAL and ATLASGAL to perform the SED fitting of G338.93-0.06, the physical properties of G338.93-0.06 revealed a class-I YSO with a relatively young core with an intermediate mass of 3.95 $M_{\odot}$, the star is at its young age of 2.426×10^{4} yrwith an effective temperature of 4.38×10^{3} K.A broader SED of the source shows mid-infrared and near-infrared excess emanating from large amounts of circum-protostellar dust. With an envelope radius of 1.058×10^{4} AU surrounding the protostar, isothermal free-fall accretion is expected to continue above the adiabatic protostar core and the density and temperature will continue to increase.

REFERENCES

1. Bedding, T. R., Mosser, B., Huber, D., Montalbán, J., Beck, P., Christensen-Dalsgaard, J., Elsworth, Y. P., García, R. A., Miglio, A., Stello, D., White, T. R., De Ridder, J., Hekker, S., Aerts, C., Barban, C., Belkacem, K., Broomhall, A. M., Brown, T. M., Buzasi, D. L. and Ventura, P. (2011). Gravity modes as a way to distinguish between hydrogen- and helium-burning red giant stars. *Nature*, *471*(7340), 608–611.
2. Benjamin, R. A., Churchwell, E., Babler, B. L., Bania, T. M., Clemens, D. P., Cohen, M., Dickey, J. M., Indebetouw, R., Jackson, J. M., Kobulnicky, H. A., Lazarian, A., Marston, A. P., Mathis, J. S., Meade, M. R., Seager, S., Stolovy, S. R., Watson, C., Whitney, B. A., Wolff, M. J. and Wolfire, M. G. (2003). GLIMPSE. I. An SIRTF Legacy Project to Map the Inner Galaxy. In *Publications of the Astronomical Society of the Pacific* (Vol. 115)..
3. Beuther, H. (2006). Physics and chemistry of hot molecular cores. *Proceedings of the International Astronomical Union*, *2*(S237), 148–154.
4. Carey, S. J., Noriega-Crespo, A.,

Mizuno, D. R., Shenoy, S., Paladini, R., Kraemer, K. E., Price, S. D., Flagey, N., Ryan, E., Ingalls, J. G., Kuchar, T. A., Pinheiro Gonçalves, D., Indebetouw, R., Billot, N., Marleau, F. R., Padgett, D. L., Rebull, L. M., Bressert, E., Ali, B. and Testi, L. (2009). MIPSGAL: A Survey of the Inner Galactic Plane at 24 and 70 μm. *Publications of the Astronomical Society of the Pacific*, *121*(875), 76–97.

5. Clarisse, N. and Sarma, A. (2019). Methanol Masers in Star-Forming Regions. *DePaul Discoveries*, *8*(1). https://via.library.depaul.edu/depaul-disc/vol8/iss1/3
6. Ellingsen, S. P. (2006). Methanol masers : Reliable tracers of the early stages of high-mass star formation. *The Astrophysical Journal*, *638*(1), 241–261.
7. Ezer, D. and Cameron, A. G. W. (1971). The evolution of hydrogen-helium stars. *Astrophysics and Space Science*, *14*(2), 399–421.
8. Fontani, F., Cesaroni, R. and Furuya, R. S. (2010). Class I and Class II methanol masers in high-mass star-forming regions. *Astronomy and Astrophysics*, *517*(8), A56.
9. Gammie, C. F., Lin, Y., Stone, J. M. and Ostriker, E. C. (2003). Analysis of Clumps in Molecular Cloud Models: Mass Spectrum, Shapes, Alignment, and Rotation. *The Astrophysical Journal*, *592*(1), 203–216.
10. Gao, Y. and Solomon, P. M. (2004). The Star Formation Rate and Dense Molecular Gas in Galaxies. *The Astrophysical Journal*, *606*(1), 271–290. https://doi.org/10.1086/382999
11. Gerola, H. and Seiden, P. E. (1978). Stochastic star formation and spiral structure of galaxies. *The Astrophysical Journal*, *223*, 129.
12. Goedhart, S., Maswanganye, J. P., Gaylard, M. J., Walt, D. J. and Van Der. (2014). Periodicity in Class II methanol masers in high-mass star-forming regions 1 I N T RO D U C T I O N. *Monthly Notices of the Royal Astronomical Society*, *437*, 1808–1820.
13. Iben, I. J. (1968). Low-Mass Red Giants. *The Astrophysical Journal*, *154*, 581.
14. Jenkins, J. L. (2013). *Observing the Sun A Pocket Field Guide*. Springer New York.
15. Lada, C. J. (1987). Star Formation: From OB Associations to Protostars. *Symposium - International Astronomical Union*, *115*, 1–18.
16. Lada, C. J., Lombardi, M. and Alves, J. F. (2010). ON THE STAR FORMATION RATES IN MOLECULAR CLOUDS. *The Astrophysical Journal*, *724*(1), 687.
17. Lada, C. J. and Wilking, B. A. (1984). THE NATURE OF THE EMBEDDED POPULATION IN THE RHO OPHIUCHI DARK CLOUD: MID-INFRARED OBSERVATIONS. *The Astrophysical Journal*, *287*, 610–621.
18. Minier, V., Burton, M. G., Hill, T., Pestalozzi, M. R., Purcell, C. R., Garay, G., Walsh, A. J. and Longmore, S. (2005). Star-forming protoclusters associated with methanol masers. *Astronomy & Astrophysics*, *429*(3), 945–960.
19. Minier, V., Ellingsen, S. P., Norris, R. P. and Booth, R. S. (2003). The protostellar mass limit for 6.7 GHz methanol masers. *Astronomy & Astrophysics*, *403*(3), 1095–1100.
20. Monnier, J. D. and Gabet, R. (2002). On the Interferometric Sizes of Young Stellar Objects. *The Astrophysical Journal*, *579*(2), 694–698.
21. Omez, A. N. A. I. G., Castro, D. E. and Wamsteker, W. (2007). *Fundamental Questions in Astrophysics* (Vol. 303).
22. Pestalozzi, M., Humphreys, E. M. L. and Booth, R. S. (2002). First SIMBA observations towards CH$_\mathsf{3}$OH masers. *Astronomy & Astrophysics*, *384*(2), L15–L18.
23. Podsiadlowski, P. (2012). The evolution of binary systems. In *Accretion Processes In Astrophysics: XXI Canary Islands*

Winter School Of Astrophysics (Vol. 9781107030190, pp. 45–88). Cambridge University Press.
24. Robitaille, T. P., Whitney, B. A., Indebetouw, R. and Wood, K. (2007). Interpreting Spectral Energy Distributions from Young Stellar Objects. II. Fitting Observed SEDs Using a Large Grid of Precomputed Models. *The Astrophysical Journal Supplement Series*, *169*(2), 328–352.
25. Robitaille, T. P., Whitney, B. A., Indebetouw, R., Wood, K. and Denzmore, P. (2006). Interpreting Spectral Energy Distributions from Young Stellar Objects. I. A Grid of 200,000 YSO Model SEDs. *The Astrophysical Journal Supplement Series*, *167*(2), 256–285.
26. Sweigart, A. V. and Gross, P. G. (1978). Evolutionary sequences for red giant stars. *The Astrophysical Journal Supplement Series*, *36*, 405.
27. Tannirkulam, A., Harries, T. J. and Monnier, J. D. (2007). The Inner Rim of YSO Disks: Effects of Dust Grain Evolution. *The Astrophysical Journal*, *661*(1), 374–384.
28. Tohline, J. E. (2002). The Origin of Binary Stars. *Annual Review of Astronomy and Astrophysics*, *40*, 349–385.
29. van der Walt, D. J., Goedhart, S. and Gaylard, M. J. (2009). Periodic class II methanol masers in G9.62+0.20E. *Monthly Notices of the Royal Astronomical Society*, *398*(2), 961–970.
30. Walsh, A. J., Macdonald, G. H., Alvey, N. D. S., Burton, M. G. and Lee, J.-K. (2003). Observations of warm dust near methanol masers. *Astronomy & Astrophysics*, *410*(2), 597–610.
31. Whitney, B. A., Wood, K., Bjorkman, J. E. and Cohen, M. (2003). Two- dimensional Radiative Transfer in Protostellar Envelopes. II. An Evolutionary Sequence. *The Astrophysical Journal*, *598*(2), 1079–1099.
32. Whitney, B. A., Wood, K., Bjorkman, J. E. and Wolff, M. J. (2003).Two- dimensional Radiative Transfer in Protostellar Envelopes. I. Effects of Geometry on Class I Sources. *The Astrophysical Journal*, *591*(2), 1049–1063.
33. Walsh, A. J., Macdonald, G. H., Alvey, N. D. S., Burton, M. G. and Lee, J.-K. (2003). Observations of warm dust near methanol masers. *Astronomy & Astrophysics*, *410*(2), 597–610.
34. Wood, D. O. S. and Churchwell, E. (1989). Massive stars embedded in molecular clouds - Their population and distribution in the galaxy. *The Astrophysical Journal*, *340*, 265.
35. Zinnecker, H. and Yorke, H. W. (2007). Toward Understanding Massive Star Formation. *Annual Review of Astronomy and Astrophysics*, *45*(1), 481–563.

36. Goedhart et al. (2014) detected G338.93-0.06 as a massive molecular cloud source with the Hartebeesthoek Radio Astronomy Observatory (HartRAO26)'s m telescope, and a 6.7 GHz methanol maser was revealed to be connected with the source. The spectral energy distribution (SED) of G338.93-0.06 was investigated, and the model was used to calculate the physical properties of the source, including stellar parameters (mass, temperature, age, radius, luminosity), envelope parameters (mass, envelope radius, accretion rate, circumstellar extinction, cavity angle), and disk parameters (mass, size, scale height, inner/outer radius). The SED fitting of G338.93-0.06 was performed using a combination of infrared data from the GLIMPSE, MIPSGAL, Hi-GAL, and ATLASGAL surveys. With a correlation coefficient of 0.6489, a power law fitting on the SED reveals a positively linked SED.